Title	Anodic oxidation of InP in KOH electrolytes
Authors	O'Dwyer, Colm;Melly, T.;Harvey, E.;Buckley, D. Noel;Cunnane, V. J.;Sutton, David;Serantoni, M.;Newcomb, Simon B.
Publication date	2002-10
Original Citation	O'Dwyer, C., Melly, T., Harvey, E., Buckley, D. N., Cunnane, V. J., Sutton, D., Serantoni, M. and Newcomb, S. B. (2002) 'Anodic Oxidation of InP in KOH Electrolytes', State-of-the-Art Program on Compound Semiconductors XXXVII (SOTAPOCS XXXVII) / Narrow Bandgap Optoelectronic Materials and Devices, 202nd ECS Meeting, Salt Lake City, Utah, 20-24 October, in Proceedings - Electrochemical Society, Vol. 14, pp. 233-240. ISBN 1-56677-306-5.
Type of publication	Conference item
Link to publisher's version	http://ecsdl.org/site/misc/proceedings_volumes.xhtml
Rights	© 2002, Electrochemical Society
Download date	2024-04-25 12:28:02
Item downloaded from	https://hdl.handle.net/10468/2883

ANODIC OXIDATION OF InP IN KOH ELECTROLYTES

C. O'Dwyer[†‡], T. Melly[†‡], E. Harvey[†‡], D. N. Buckley[†‡], V. J. Cunnane[‡*],
M. Serantoni[‡], D. Sutton[‡], and S. B. Newcomb[‡]

[†] *Dept. of Physics, University of Limerick, Ireland*
[‡] *Materials and Surface Science Institute, University of Limerick, Ireland*
[*] *Dept. of Chemistry and Environmental Science, University of Limerick, Ireland*

ABSTRACT

The anodic behavior of InP in 1 mol dm^{-3} KOH was investigated and compared with its behavior at higher concentrations of KOH. At concentrations of 2 mol dm^{-3} KOH or greater, selective etching of InP occurs leading to thick porous InP layers near the surface of the sustrate. In contrast, in 1 mol dm^{-3} KOH, no such porous layers are formed but a thin surface film is formed at potentials in the range 0.6 V to 1.3 V. The thickness of this film was determined by spectroscopic ellipsometry as a function of the upper potential and the measured film thickness corresponds to the charge passed up to a potential of 1.0 V. Anodization to potentials above 1.5 V in 1 mol dm^{-3} KOH results in the growth of thick, porous oxide films ($\sim$ 1.2 μm). These films are observed to crack, *ex-situ*, due to shrinkage after drying in ambient air. Comparisons between the charge density and film thickness measurements indicate a porosity of approximately 77% for such films.

INTRODUCTION

III-V semiconductors are widely used in optoelectronic devices as well as in high power and high speed electronic devices. Studies of the anodic growth of films on III-V semiconductors such as InP [1] and GaAs [2] have stemmed from their potential use as passivating layers and as insulating layers in metal-insulator-semiconductor (MIS) devices. The nature of the anodic film formed is very much dependant on the details of the electrochemical procedure. For example anodic treatments on InP in sulphur-containing electrolytes can result in passivated surfaces with increased stability [3,4] or thicker porous films in which cracking of the anodically grown surface film occurs [5-8]. Photoluminescence measurements of photo-anodically grown films on GaN have indicated the passivating nature of the layers [9] grown and metal-oxide-semiconductor (MOS) structures using photo-electrochemically formed oxide layers on GaN have been fabricated [10]. However, depending on the anodization details, cracking of the anodic oxide film can also occur for the case of GaN. [9]

Thus, the nature of anodic films on compound semiconductors, their structure and composition, and the relationship to growth conditions are important, both from a

fundamental and a technological point of view. In this paper, we report the anodic oxidation of InP in 1 mol dm^{-3} KOH and contrast the morphology with that obtained after anodization in higher concentrations of KOH.

EXPERIMENTAL

The working electrode consisted of polished (100)-oriented monocrystalline sulphur doped n-InP with a carrier concentration of approximately 3×10^{18} cm^{-3}. An ohmic contact was made by alloying indium to the InP sample and the contact was isolated from the electrolyte by means of a suitable varnish. The electrode area was typically 0.2 cm^2. Anodization was carried out in KOH electrolytes varying in concentration from 1 – 5 mol dm^{-3}. A conventional three electrode configuration was used employing a platinum counter electrode and saturated calomel reference electrode (SCE) to which all potentials are referenced. Prior to immersion in the electrolyte, the working electrode was dipped in a 3:1:1 H_2SO_4:H_2O_2:H_2O etchant and rinsed in deionized water. All of the electrochemical experiments were carried out at room temperature and in the dark.

A CH Instruments Model 650A Electrochemical Workstation interfaced to a Personal Computer (PC) was employed for cell parameter control and for data acquisition. Ellipsometric measurements of thin surface films were made with a J.A. Wollam M2000 Spectroscopic Ellipsometer. The surfaces of the anodized samples were examined using a Joel JSM 840 scanning electron microscope (SEM). Cross-sectional slices were thinned to electron transparency using standard focused ion beam milling procedures by means of a FEI 200 FIBSIMS workstation. The transmission electron microscopy (TEM) and electron diffraction was performed using a JEOL 2010 TEM operating at 200 kV. A Princeton Gamma-Tech digital spectrometer was used with the SEM for Energy Dispersive X-ray analysis (EDX).

RESULTS AND DISCUSSION

Thin Surface Layers

Cross-sectional TEM micrographs of n-InP electrodes anodized in 3 mol dm^{-3} and 1 mol dm^{-3} KOH electrolytes are shown in Fig 1a and Fig. 1b respectively. The TEM image shown in Fig. 1a was acquired after an electrode was anodized from 0.0 V to 0.68 V at a scan rate of 2.5 mV s^{-1}. The micrograph in Fig. 1b was acquired after an electrode was subjected to a potential sweep from 0.0 V to 1.3 V. As is apparent from the micrographs, the anodic oxidation processes are remarkably different in the two different concentrations of KOH. Anodization in 3 mol dm^{-3} KOH electrolytes results in the formation of porous InP layers. The layer typically extends over 750 nm into the bulk substrate and there is no evidence of an anodic film present on the surface, although TEM electron diffraction measurements indicate that In_2O_3 exists within the pores [11]. Detailed characterization of these layers can be found elsewhere [11]. Similar porous layers are obtained in 2 mol dm^{-3} and 5 mol dm^{-3} KOH.

In contrast, after a similar potential sweep in a 1 mol dm^{-3} KOH electrolyte no porous structure is evident on the electrode; rather the InP electrode is covered with a relatively compact surface film with thickness of ~ 25 nm as indicated in Fig. 1b. Electron diffraction data obtained for the surface film, indicates that it is composed of a mixture of In$_2$O$_3$ and InPO$_4$ and it is apparent from the intensity of the respective diffraction rings that the In$_2$O$_3$ is the dominant phase. This is in agreement with previous reports on the composition of anodic films on InP [1,12].
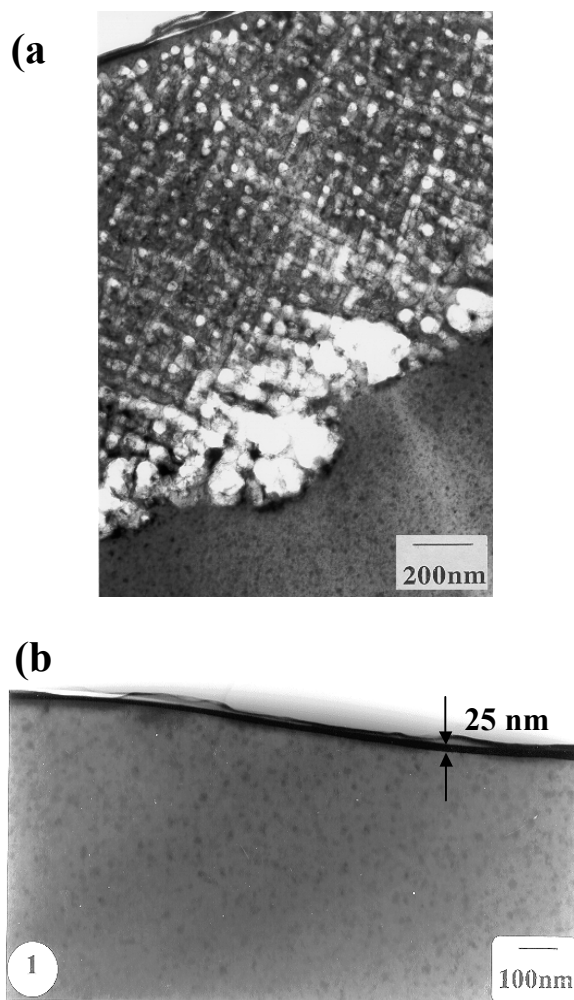
Fig. 1 Bright field through focal TEM micrographs of InP electrode cross-sections after a potential sweep from (a) 0.0 V to 0.68 V (SCE) at a scan rate of 2.5 mV s^{-1} in 3 mol dm^{-3} KOH and (b) 0.0 V to 1.3 V at a scan rate of 10 mV s^{-1} in 1 mol dm^{-3} KOH.

The current vs. potential characteristics of InP electrodes in 3 mol dm^{-3} are shown in Fig. 2 for a series of scan rates in the range 1 mV s^{-1} to 10 mV s^{-1}. The potential was scanned from 0.0 V to a range of higher potentials: the upper potential chosen depended on the scan rate. Considering the current vs. potential curve (Fig. 2(b)) for a scan rate of 2.5 mV s^{-1}, it is noted that very little current flow is observed until a potential of 0.3 V is reached after which a sharp rise in current is noted. The current reaches a peak at 0.45 V after which it falls off to low values. A secondary peak is also observed which becomes fully resolved at higher scan rates. Similar curves (Fig. 2(a) – (e)) are obtained for higher and lower scan rates but peak currents are higher and values of potential shift to more

anodic potentials as the scan rate is increased. The charge passed during each full potential sweep was estimated by numerical integration of the current with respect to time. It appears that the variation in scan rate does not appreciably alter the quantity of charge passed during a potential sweep, and a value close 1.4 C cm^{-2} was measured for each scan rate.
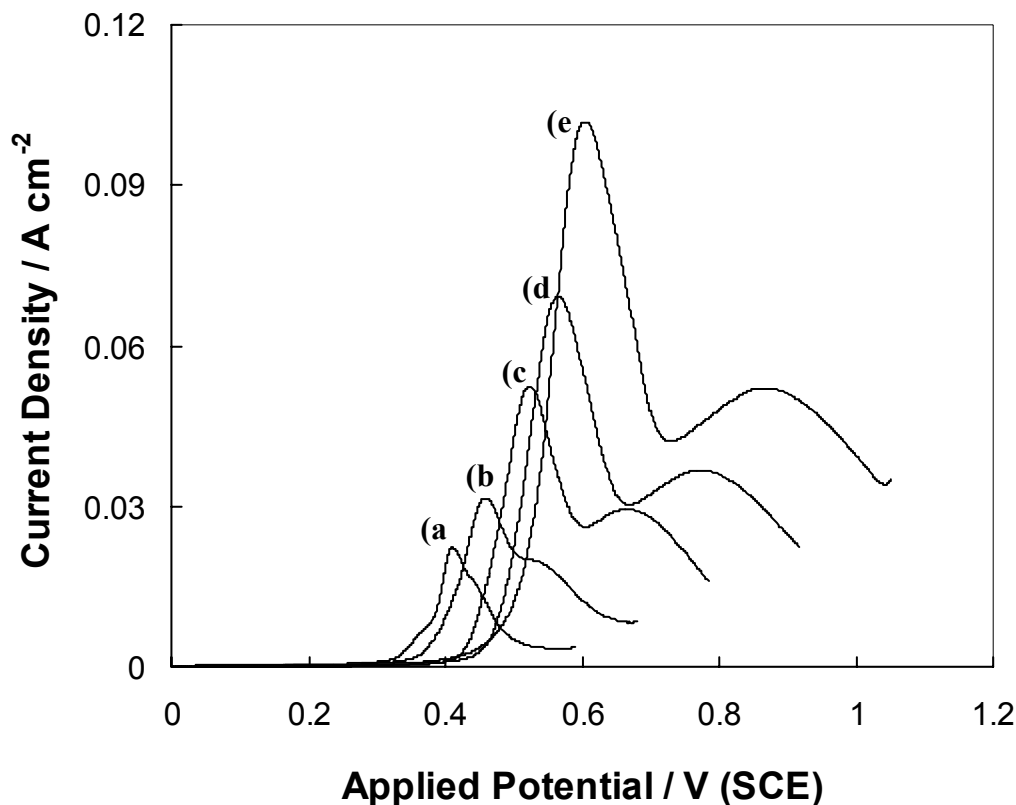
Fig. 2 Linear potential sweep of InP electrodes in 3 mol dm^{-3} KOH solution at scan rates of (a) 1 mV s^{-1}, (b) 2.5 mV s^{-1}, (c) 5 mV s^{-1}, (d) 7.5 mV s^{-1} and (e) 10 mV s^{-1}.

Fig. 3 shows the typical current vs. potential response of InP electrodes in a 1 mol dm^{-3} aqueous KOH electrolyte at scan rates in the range 2.5 mV s^{-1} to 10 mV s^{-1}. The potential was scanned from 0.0 V to 2.5 V (SCE) in each case. Considering the current vs. potential curve (Fig. 3(a)) for a scan rate of 2.5 mV s^{-1}, it is noted that very little current flow is measured in the potential range 0.0 V to 0.6 V. As the potential is increased further, however, the current density begins to increase rapidly from a value of 0.5 mA cm^{-2} at 0.8 V to a peak current density of 9 mA cm^{-2} at 1.25 V. Above a potential of 1.25 V, the current density decrease to a value of 7 mA cm^{-2} at 1.55 V. Further increases in potential result in a gradual decrease in current density.

The shape of the current vs. potential curves is similar for all scan rates. While the peak current density increases with increasing scan rate, the potential of the current peak is found to occur at slightly lower potentials.
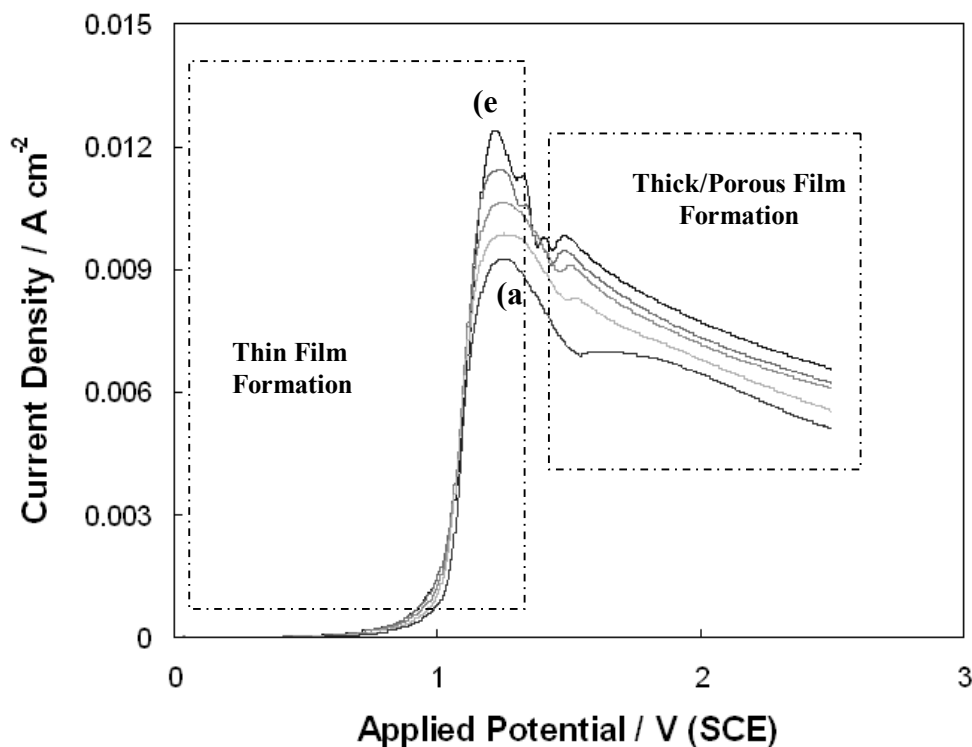
Fig. 3 Linear potential sweeps of InP electrodes in 1 mol dm^{-3} KOH solution from 0.0 V to 2.5 V (SCE) at scan rates of (a) 2.5 mV s^{-1}, (b) 3.75 mV s^{-1}, (c) 5 mV s^{-1}, (d) 7.5 mV s^{-1} and (e) 10 mV s^{-1}.

Spectroscopic ellipsometry was employed to characterize the growth and thickness variation of the oxide formed on InP in 1 mol dm^{-3} KOH. A series of potential sweeps were carried out from 0.0 V to upper potential limits in the range of 0.6 V to 1.3 V. After anodization, the electrode was rinsed and the ellipsometric data was acquired *ex-situ* with incident angles ranging from $60^0 - 80^0$ in the wavelength range $200 - 800$ nm. Film thicknesses were determined, assuming an In$_2$O$_3$ layer and the values obtained are plotted in Fig. 4 against the upper limit of the potential sweep. The thickness of a theoretical surface film based on the charge passed is overlaid for comparison. These values were derived from Faraday's law using the cumulative charge passed to each upper potential value and assuming an 8-electron electrochemical process.

From the ellipsometric measurements, a thickness of 26.5 nm was measured for the thickness of the anodic film after a potential sweep to 1.3 V and this value is in agreement with the film thickness as measured using TEM (~25 nm). Comparing the ellipsometrically measured thickness values with the corresponding theoretical film thickness based on charge, it is observed that there is reasonable agreement up to a potential of ~ 1.0 V. Thereafter, the two curves diverge as the charge-based thickness estimates increase sharply indicating that, above 1.0 V, most of the charge passed is not involved in the formation of a surface film.
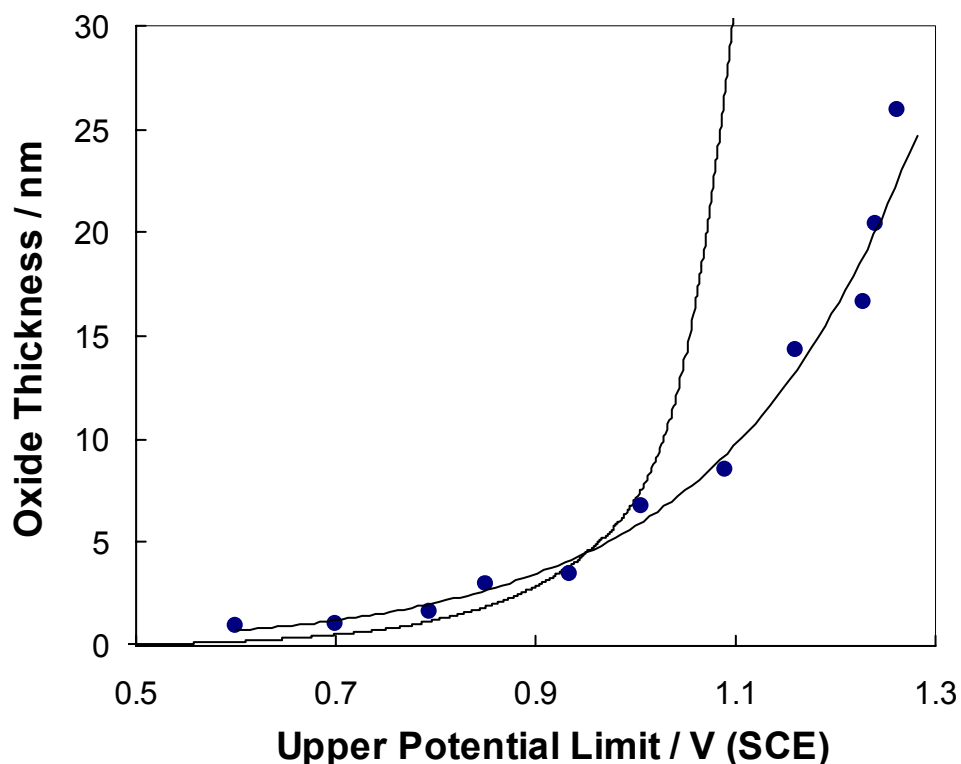
Fig. 4 (•) Ellipsometrically measured film thickness as a function of the upper limit of the potential sweep. (——) Variation of the theoretical film thickness based on the charge passed during the potential sweep.

Porous Film Formation and Cracking

Both scanning electron microscopy and focused ion beam microscopy have been employed to characterize the porous nature of anodic films formed at potentials above 1.5 V in 1 mol dm^{-3} KOH. Fig. 5a is a plan view scanning electron micrograph of the surface film after a potential sweep to 2.5 V. The image was acquired *ex-situ* after drying in ambient air. As is evident from the micrograph, the surface film is severely cracked. It has been demonstrated through the use of time-lapse optical microscopy that the film is initially not cracked when the electrode is removed from the cell but that cracking occurs during film drying. Clearly the surface cracking is not a characteristic of the film *in-situ* during anodization but rather occurs *ex-situ* after drying in ambient air. Thus, it does not necessarily imply strain relief in the film as it is being formed. Quantitative EDX studies and TEM electron diffraction have shown the film to be composed primarily In$_2$O$_3$.

Quantitative estimates of the degree of shrinkage were made. A series of lines were drawn on the micrographs and the lengths of the segments where a line crossed the cracks were measured. The sum of the lengths of these segments on a line expressed as a fraction of the total length of the line gives the fractional (linear) shrinkage. From measurements on a series of such lines, an average linear shrinkage of 25% was obtained.

Focused ion beam milling was also used to examine the cross-sectional structure of the cracked, highly porous film. After bulk milling and supplementary clean-up cuts, the

cross-sectional structure of the cracked, porous film was imaged and is shown in Fig. 5b. The highly porous nature of the film is evident and shrinkage of the film due to drying resulted in some segments becoming separated from the bulk substrate providing further evidence that shrinkage occurs both vertically and laterally. Calculation of the quantity of charge passed during anodization to 2.5 V [1.35 C cm^{-2}] yields a theoretical estimate of 0.338 μm for the film thickness assuming a compact film of In_2O_3 is formed. The measured film thickness, however, was found to be ~ 1.2 μm. The ratio of the estimated thickness of a compact film to the measured film thickness gives a value of ~ 0.3. Allowing for shrinkage of 25%, an estimate for the percentage porosity of ~ 77% is obtained. This is similar to the values quoted by Harvey et al. for cracked, porous anodic sulfide films on InP [6].
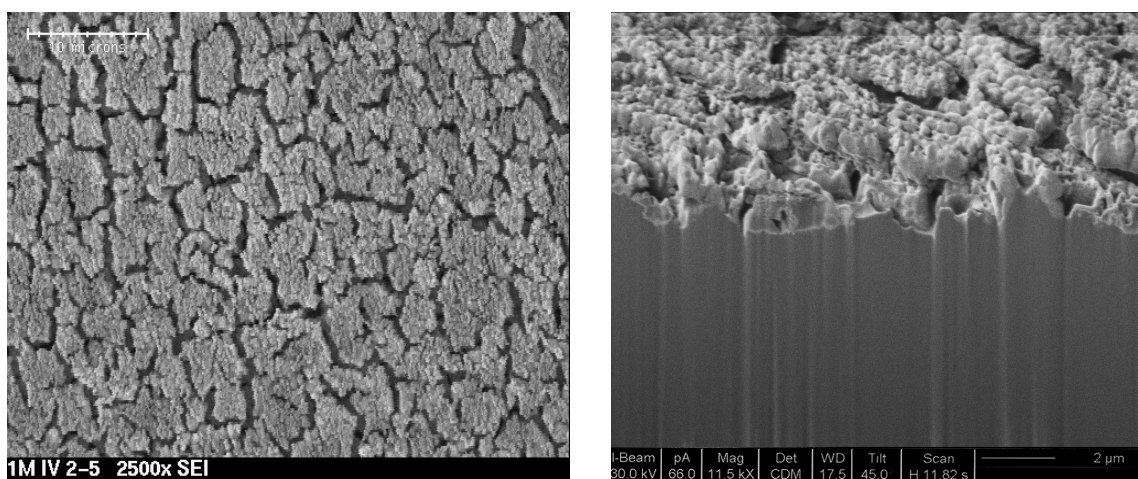
Fig. 5 (a) Plan view SEM micrograph of the InP surface film after a potential sweep from 0.0 V to 2.5 V (SCE) at a scan rate of 10 mV s^{-1} in 1 mol dm^{-3} KOH showing the nature of film cracking after shrinkage. (b) Milled cross sectional focused ion beam image of (a) showing the highly porous anodic film.

The thicker porous films observed to form in the potential range 1.5 – 2.5 V contain a high volume fraction of electrolyte during anodization and so an efficient pathway for the ion transport. The detailed growth mechanism has not been elucidated but porous In_2S_3 layers formed during anodization of InP in $(NH_4)_2S$ are believed to form by a dissolution-precipitation mechanism. A similar mechanism may be involved in KOH.

CONCLUSIONS

Although the linear potential sweeps obtained for InP in 1 mol dm^{-3} KOH are qualitatively similar to those obtained in higher concentrations of KOH, the processes occurring during anodization are markedly different. At concentrations of 2 mol dm^{-3} KOH or greater, selective etching of InP occurs leading to thick porous layers near the surface. In contrast, in 1 mol dm^{-3} KOH, no such porous layers are formed but a thin surface film is formed at potentials in the range 0.6 V to 1.3 V. The thickness of this film was determined by spectroscopic ellipsometry as a function of the upper potential and the measured film thickness corresponds to the charge passed up to a potential of 1.0 V.

Anodization to potentials above 1.5 V in 1 mol dm^{-3} KOH results in the formation of thick, porous films. Cracking of such films is noted to occur *ex-situ* due to shrinkage during drying in ambient air and does not occur during the anodization procedure. From a comparison of the charge density and the measured thickness, the porosity of these films was estimated as 77%. It appears that this structure provides an easy access pathway for the diffusion of ions between the substrate and the bulk electrolyte so that film growth is not inhibited.

REFERENCES

[1] I. Gerard, N. Simon and A. Etcheberry, *Appl. Surf. Sci.*, **175-176**, 734 (2001)

[2] P. Schmuki, G.I. Spoule, J.A. Bardwell, Z.H. Lu and M.J. Graham, *J. Appl. Phys.*, **79**, 7303 (1996)

[3] J. Yota and V.A. Burrows, *J. Vac. Sci. Technol. A*, **11**, 1083 (1993)

[4] Z.S. Li, X.Y. Hou, W.Z. Cai, W.Wang, X.M. Ding and X. Wang, *J. Appl. Phys.,* **78**, 2764 (1995)

[5] L.J. Gao, J.A.Bardwell, Z.H. Lu, M.J. Graham and P.R. Norton, *J. Electrochem. Soc.*, **142**, L14 (1995)

[6] E. Harvey, D.N. Buckley, S.N.G. Chu, D. Sutton and S.B. Newcomb, *J. Electrochem. Soc.*, **149** (Sept. 2002)

[7] D.N. Buckley, E. Harvey and S.N.G. Chu, *Chemical Monthly*, **133**, 785 (2002)

[8] E. Harvey and D.N. Buckley, in *Proceedings of the 32nd State-of-the-Art Program on Compound Semiconductors*, R.F. Kopf, A.G. Baca and S.N.G. Chu, Editors, PV 2000-1, p. 265, The Electrochemical Society, Proceedings Series, Pennington, NJ (2000)

[9] L.-H. Peng, C.-H. Liao, Y.-C. Hsu, C.-S. Jong, C.-N. Huang, J.-K. Ho, C.-C. Chiu and C.-Y. Chen, *Appl. Phys. Lett.*, **76**, 511 (2000)

[10] T. Rotter, R. Ferretti, D. Mistele, F. Fedler, H. Klausing, J. Stemmer, O.K. Semchinova, J. Aderhold and J. Graul, *J. Crystal Growth,* **230**, 602 (2001)

[11] E. Harvey, C. O'Dwyer, T. Melly, D.N. Buckley, V.J. Cunnane, D. Sutton, S.B. Newcomb and S.N.G. Chu, in *Proceedings of the State-of-the-Art Program on Compound Semiconductors XXXV*, P. -C. Chang, S. N. G. Chu and D. N. Buckley, Editors, PV 2001-2, p. 87, The Electrochemical Society, Proceedings Series, Pennington, NJ (2001)

[12] O. Pluchery, J. Eng Jr., R.L. Opila and Y.J. Chabal, *Surf. Sci.*, **502**, 75 (2002)